



**HAL**  
open science

## Low-resolution spectroscopy mode for CASTLE telescope with a composite grism

Eduard Muslimov, Jean-François Sauvage, Simona Lombardo, Damir  
Akhmetov, Danila Kharitonov

► **To cite this version:**

Eduard Muslimov, Jean-François Sauvage, Simona Lombardo, Damir Akhmetov, Danila Kharitonov.  
Low-resolution spectroscopy mode for CASTLE telescope with a composite grism. SPIE Astronomical  
Telescopes + Instrumentation, Jul 2022, Montréal, Canada. 10.1117/12.2628688 . hal-03937312

**HAL Id: hal-03937312**

**<https://hal.science/hal-03937312>**

Submitted on 25 Jan 2023

**HAL** is a multi-disciplinary open access archive for the deposit and dissemination of scientific research documents, whether they are published or not. The documents may come from teaching and research institutions in France or abroad, or from public or private research centers.

L'archive ouverte pluridisciplinaire **HAL**, est destinée au dépôt et à la diffusion de documents scientifiques de niveau recherche, publiés ou non, émanant des établissements d'enseignement et de recherche français ou étrangers, des laboratoires publics ou privés.

# Low-resolution mode for CASTLE telescope with a composite grism

Eduard Muslimov<sup>a,b,c</sup>, Jean-Francois Sauvage<sup>b</sup>, Simona Lombardo<sup>b</sup>, Damir Akhmetov<sup>c</sup>, and Danila Kharitonov<sup>c</sup>

<sup>a</sup>NOVA Optical IR Instrumentation Group at ASTRON Oude Hoogeveensedijk 4, 7991 PD Dwingeloo, The Netherlands

<sup>b</sup>Aix Marseille Univ, CNRS, CNES, LAM, Marseille, France

<sup>c</sup>Kazan National Research Technical University named after A.N. Tupolev KAI, 10 K. Marx, Kazan, Russia, 420111

## ABSTRACT

The CASTLE is a small robotic telescope designed for the observations of ultra-low surface brightness objects and the search and detection of transient objects. The telescope is designed and built at Laboratoire d'Astrophysique de Marseille and will be installed at the Calar Alto Observatory. In the present work we consider a possibility to implement a low-resolution slitless spectroscopy mode for CASTLE in order to provide a fast spectrum of the transient immediately after the first detection. Such an additional observation mode could be realized by introduction of a grism in the pre-focal position at the filter wheel. The grism can create spectral images with a minimal decentering and a small defocusing, so the same detector and focusing mechanism can be used. Use of a volume-phase holographic grating as the main dispersing part of the grism allows to reach a high diffraction efficiency together with the low level of scattered light. The value of the spectral resolving power is  $R=163-698$  over the extended spectral range of 350-950 nm, while telescopes nominal  $f/\#=2.5$  is maintained and an extended field of view of  $9^{\circ} \times 14'$  is covered. Due to the limitations set by the telescope optical design the grism will be placed in a converging beam far from the pupil, so that its aberrations and diffraction efficiency will vary notably across the clear aperture. In order to compensate for these variations we consider using a composite holographic component, which represents a mosaic of zones. In each of them such parameters of the hologram as the photosensitive layer thickness, refraction index modulation depth and aberrations of the recording wavefronts can be optimized separately. We estimate the performances of such an innovative element and compare it with that of an ordinary grism. The comparison demonstrates gain up to a factor of 3 in the image quality and up to a factor of 4.2 in the diffraction efficiency.

**Keywords:** Low-resolution spectroscopy, Volume-phase hologram, Composite hologram, Schmidt telescope, Diffraction efficiency, Aberration correction

## 1. INTRODUCTION

The Calar Alto Schmidt-Lemaître Telescope (CASTLE) is a small sized telescope highly optimized for the detection of extremely faint and extended astrophysical objects. The telescope will be installed at the Calar Alto observatory (in Almeria, Spain). The telescope design is based on such innovative technologies as freeform mirrors and curved sensors. Thanks to these features the telescope will be able to cover a large field of view with a uniformly high image quality and provide a point spread function (PSF) with low wings, which is essential for some science applications.

Considering its characteristics, CASTLE will be a tool for new discoveries in the domain of low surface brightness (LSB) and the transient search and detection. The large field of view will be highly beneficial to search for gravitational wave optical counterparts, gamma ray bursts, neutrinos and fast radio bursts sources.

---

Further author information: (Send correspondence to E.M.)

E-mail: muslimov@astron.nl

The fast readout provided by its detector will also allow for the detection of transneptunian or trojan objects occultation in front of bright stars.<sup>1</sup>

The telescope could benefit from a spectroscopic mode, which would provide much more valuable information about the observed objects. However, coupling a spectral instrument with such a compact, fast and wide-field telescope is a very challenging task from both optical and mechanical standpoints. One of attractive prospects would be to implement a slitless low-resolution spectroscopy mode like it was done in Galex.<sup>2</sup> In such a design there is no need in additional spatial filters or relay optics and the spectrograph can use the same detector, as in the main imaging mode. The only addition to the optical design would be a grism, mounted in a converging beam in pre-focal position. Although, the grism would have to deal with a fast beam and extended field of view, so the incidence angles would vary significantly across the aperture and field of view (FoV), thus introducing notable aberrations and variation of the diffraction efficiency (DE).

However, we believe that this concept is still applicable for the CASTLE case. A possible solution is in use of a composite holographic element.<sup>3</sup> Such an element is stitched from a number of zones, where the hologram parameters can be optimized independently. This approach allows to increase the number of optimization variables drastically and account for the local variations of the hologram aberrations and DE. So, in the present paper we consider a possibility to apply the composite hologram to implement a low-resolution slitless spectroscopy mode at CASTLE telescope.

## 2. HOSTING TELESCOPE

CASTLE has an off-axis fully reflective Schmidt design, composed of a freeform primary mirror of 376 mm, acting as a Schmidt corrector plate, a flat secondary and a spherical tertiary (see Fig. 1). This design is known for a high image quality over a large FoV.<sup>4</sup> It has a curved focal surface, which was considered as its' downside for a long time. But nowadays it can be corrected in a straightforward way - by using a curved sensor.<sup>5,6</sup>

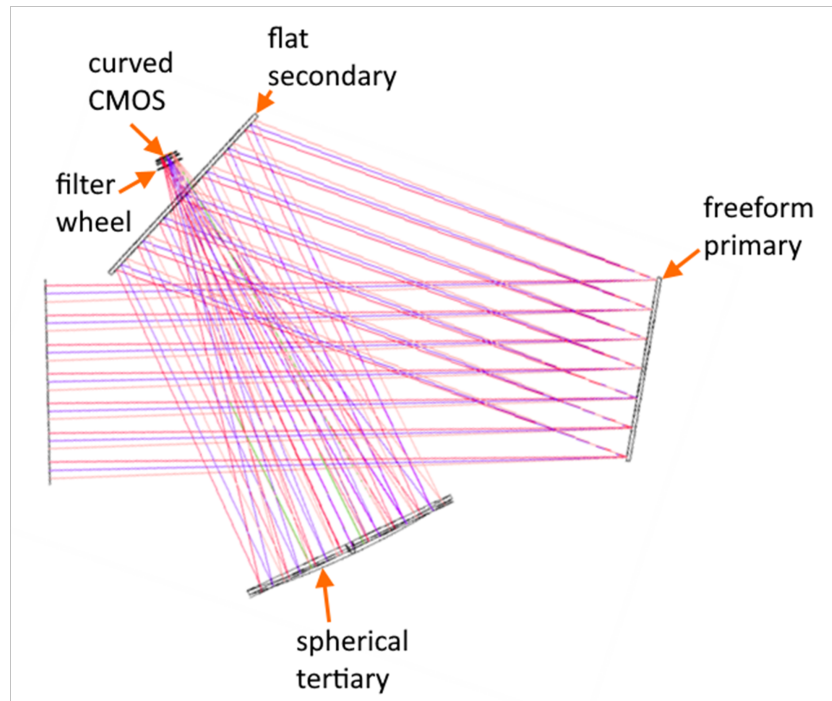


Figure 1. General view of the CASTLE telescope optical design.

The advantages of such telescope come from its unique design that combines:

- the wide field of view of a Schmidt telescope,

- the removal of supporting spiders and related diffraction effects,
- the removal of field flattening optics provided by the usage of a curved sensor to match its curved focal surface.

All these elements contribute to generate a PSF with very low level wings, uniform across the full field of view, and to effectively suppress ghost reflections, a capability that was verified by performing end-to-end photon Monte Carlo simulations<sup>1</sup> with the PhoSim software.<sup>7</sup> The detector unit will have a science graded curved CMOS sensor (back-side illuminated to increase the Quantum Efficiency up to 80%). The telescope will be equipped with  $g$ ,  $r$  and wide-band  $g+r$  (luminance filter) filters for its science applications and the facility will be robotic.

The nominal telescope design defines the initial data for the dispersing element development. It should fit on the telescope filter wheel and be able to operate with the existing focusing mechanism, which means, that the grism can't be closer than 49 mm to the secondary mirror and the detector, refocused on the spectral image can't be further than 115 mm from the mirror. The field of view in the spectroscopic mode can't cover the entire FoV of CASTLE, but must be large enough to study extended objects. Also, we have to find a compromise between the linear dispersion and field coverage to fit the spectral image on the existing detector. The spectral resolving power should be typical for this spectroscopic modes.<sup>8</sup> Finally, we can crop the longest wavelengths, where the detector's sensitivity is relatively low. The key parameters for the spectrograph design derived from the above-listed considerations are summarized in Table 1.

Table 1. Main design parameters.

F-ratio	2.5
Focal length, mm	889
Full FoV, °	2.36x1.56
Full spectral range, nm	350-1100
Spectroscopy mode FoV, arcmin	9x14
Spectroscopy mode range, nm	350-950
Target spectral resolving power	400

### 3. SPECTROGRAPH DESIGN

The algorithm of the composite holographic element design is similar to that described in the previous works.<sup>3,9</sup> The grism is mounted in 39.6 mm in front of the detector's window as it is shown in Fig. 2. It was found that in order to achieve the best image quality and more uniform DE distribution the grism surfaces should be curved. It is logical to use surfaces concentric to the beam in the field center as the starting point. The radii values obtained after the optimization are 83.2 and 41.7 mm for the first and second surface, respectively.

The composite hologram is imposed on the first surface of the grism. It represents a volume-phase hologram composed of 3 zones. The hologram is recorded at 532 nm with two coherent point sources as it is shown in Fig. 3. The polar coordinates of the sources with respect to the hologram surface vertex are  $(79.415\text{mm}, 1.908^\circ)$  and  $(77.495\text{mm}, 8.549^\circ)$ . A deformable mirror (DM) is set up after one of the sources to create an aberrated recording wavefront. The DM diameter is 16 mm and its' shape is described by the Zernike polynomials.<sup>10</sup> We use only the ZY-symmetrical polynomials up to the 4<sup>th</sup> order.

The substrate is made of BK7 glass and its' surfaces are tilted to restore the image centering. So, the substrate represents a spherical wedge with 7 mm central thickness and  $9.77^\circ$  wedge angle. Also, the first surface is tilted by  $0.63^\circ$  with respect to the incident beam at the FoV center.

The zones are recorded separately one after another (e.g. with use of a mask), so the DM settings, the exposure and the photosensitive layer thickness can be controlled independently in each zone. So, the optimal

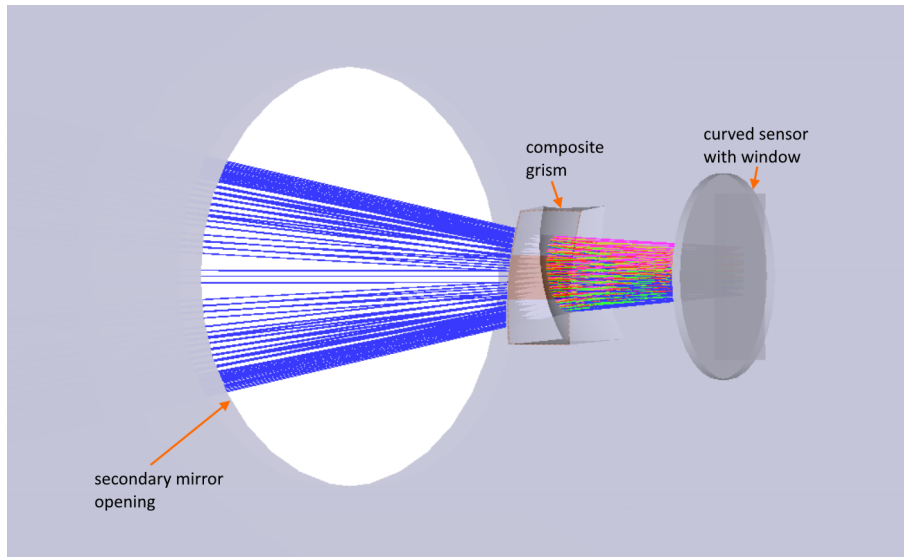


Figure 2. Composite grism mounted on the telescope filter wheel for the low-resolution spectroscopy mode.

values of these parameters vary from zone to zone. The values found with numerical optimization are summarized in Table 2. Note, that the hologram structure parameters are limited by technological feasibility, but also, by presumptions of the coupled waves theory,<sup>11</sup> which requires the structure to be thick with respect to the working wavelength. The table shows that the found values are reachable, but also that the hologram reconstruction conditions vary across its' surface notably.

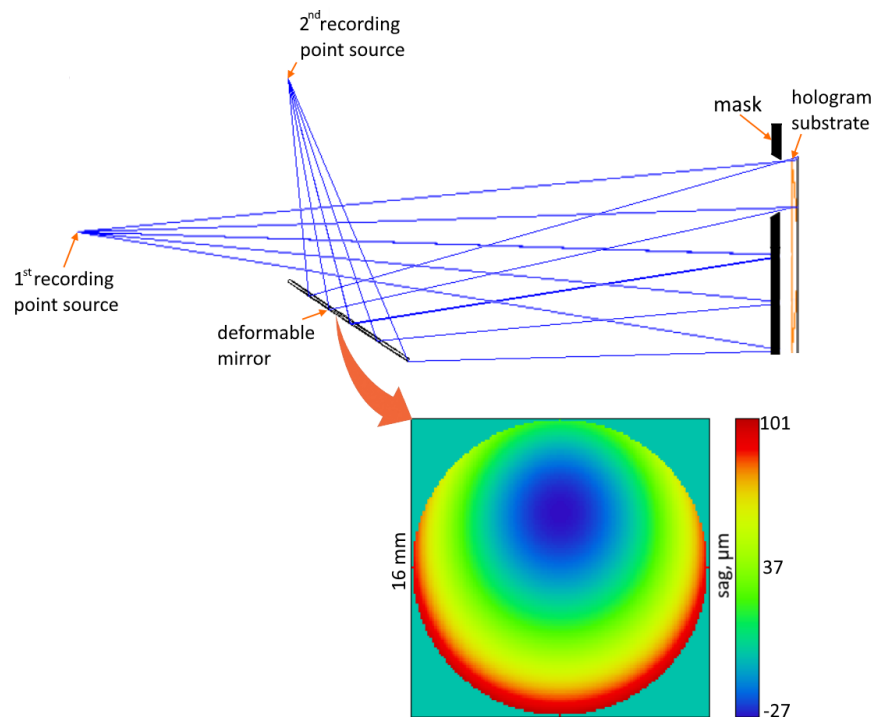


Figure 3. Composite hologram recording setup schematic.

Table 2. Design parameters of the composite grism.

Zone	Bottom	Middle	Top
DM PTV sag, $\mu m$	151	128	132
Thickness, $\mu m$	25	25	30
Modulation depth	0.0085	0.0088	0.0073

#### 4. PERFORMANCE ANALYSIS

To assess the composite grism performance we use the spot diagrams and instrument functions, based on ray-tracing and numerical convolution, and diffraction efficiency calculations, based on the Kogelnik's theory.<sup>11</sup> One must keep in mind that both of the metrics depend on the same parameters - the incidence angles in the recording and operation setups, so the models used for calculations must be coherent. Also, we have to accept a number of presumptions: the high-order aberrations of the recording wavefronts don't affect the DE variation, the conical diffraction effect is negligible, the contribution of higher diffraction orders is small and the irradiation is unpolarized.

##### 4.1 Image quality

The key metric for the image quality optimization and control is the size of the spot diagrams. The diagrams for the optimized composite grism are shown in Fig. 4. The root-mean-square (RMS) radii of the diagrams vary between  $21.8 - 33.8\mu m$ ,  $16.3 - 21.4\mu m$  and  $19.1 - 37.5\mu m$  for 350, 650 and 950 nm, respectively.

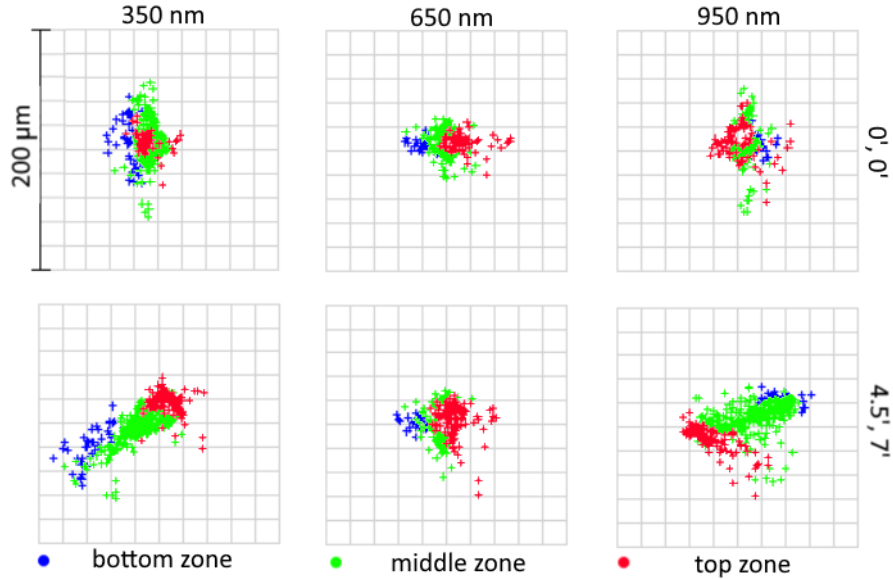


Figure 4. Spot diagrams of the slitless spectrograph.

To estimate the spectral resolving power we compute the instrument functions. With a pessimistic assumption the seeing is  $2''$ , which corresponds to  $8.7\mu m$  at the focal plane. Convoluting this spot with the PSF cross-section we obtain the instrument functions shown in Fig. 5. The full width at half maximum (FWHM) varies from center (solid lines) to corner (dashed lines) of the FoV and equals to  $15.2 - 27\mu m$ ,  $11.7 - 13.4\mu m$  and  $17.3 - 27\mu m$  for 350, 650 and 950 nm, respectively. With the spectral image length of  $7.54 mm$  the reciprocal linear dispersion is  $79.6 nm/mm$ , so the corresponding spectral resolving power  $R$  is 287-163, 698-610 and 690-442.

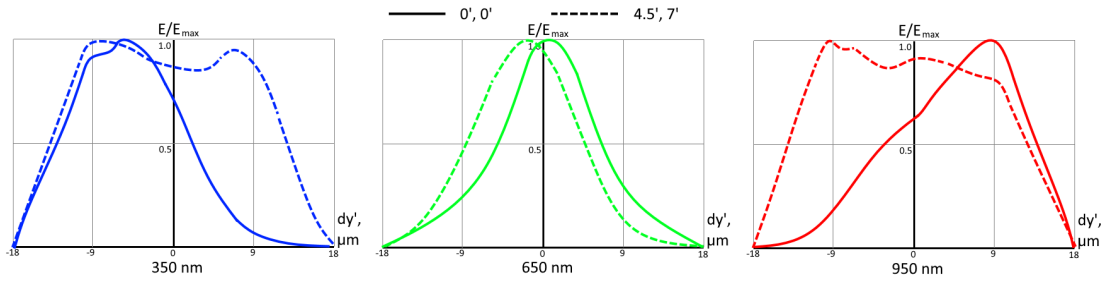


Figure 5. Instrument functions of the slitless spectrograph for  $8.7 \mu m$  object width ( $2''$  seeing).

Thus, the spectrograph provides a good aberration correction relatively uniform across the FoV. The spectral resolving power is above the target value for the most of the wavelengths, though towards the shortwave edge it notably decreases, which is expectable for a low-dispersion aberration limited system.

## 4.2 Diffraction efficiency

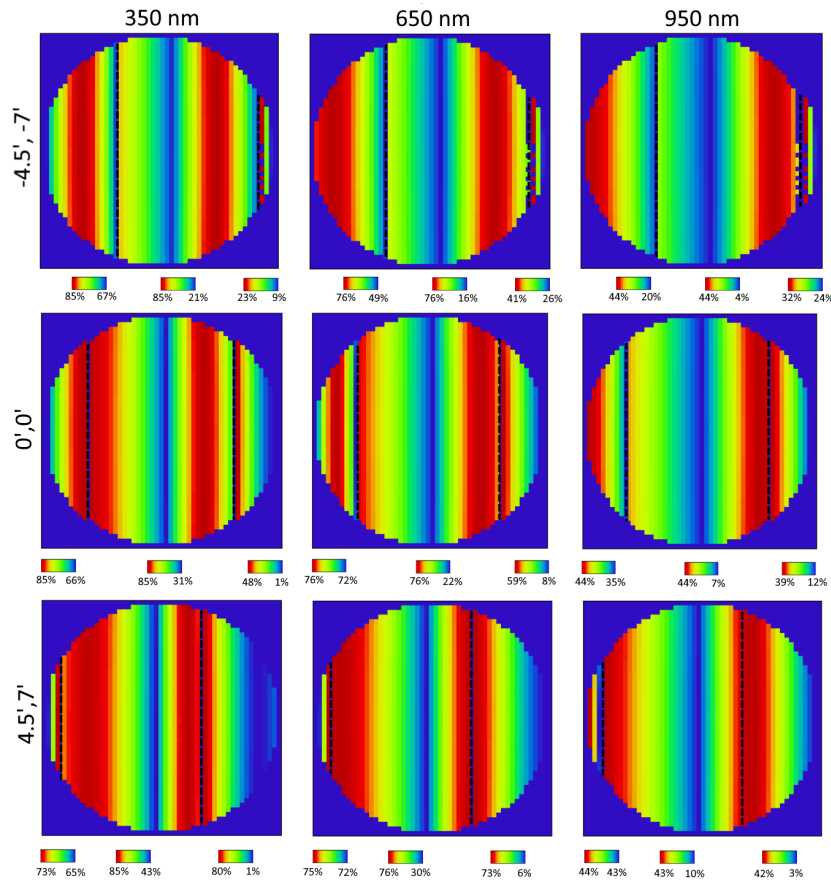


Figure 6. Diffraction efficiency distribution over the hologram surface, field of view and spectral range.

The diffraction efficiency is optimized and computed with a macro, implementing the coupled waves theory equations. The maps, showing the DE distribution over the aperture, field of view and spectral working range are shown in Fig. 6. Note, that the maximum and minimum values for each zone are different, so the colorbars are defined for each zone separately. This implies that the DE distribution experience a discontinuity as the

ray moves from one zone to another. However, this happens relatively far from the focal plane, so the rays are meshed and the irradiation distribution in the image will be smooth. Also, this effect depends only on the instrument's parameters, so it should be calibratable.

The RMS values over the aperture accounting for number of rays passing through each zone are presented in Table 3

Table 3. Diffraction efficiency values.

	350 nm	650 nm	950 nm
-4.5', -7'	63.01%	54.31%	28.04%
0', 0'	63.65%	56.22%	29.52%
4.5', 7'	64.13%	56.91%	30.25%

The values of DE, obtained here are lower than those of a typical grism mounted in a parallel beam, but they are relatively high for a component working with such a fast beam, extended FoV and wide spectral range. In order to demonstrate it, in the next section we compare the achieved performance with that of a classical grism.

### 5. PERFORMANCE COMPARISON

By a classical grism we imply here an element composed of a prism with flat surfaces and a flat volume-phase grating. The grating is recorded in a single exposure without any auxiliary optics. However, we assume that it is recorded by two point sources at finite distances. Otherwise the grism aberrations in the converging beam become too large. We keep the same key parameters and optimization settings for this case.

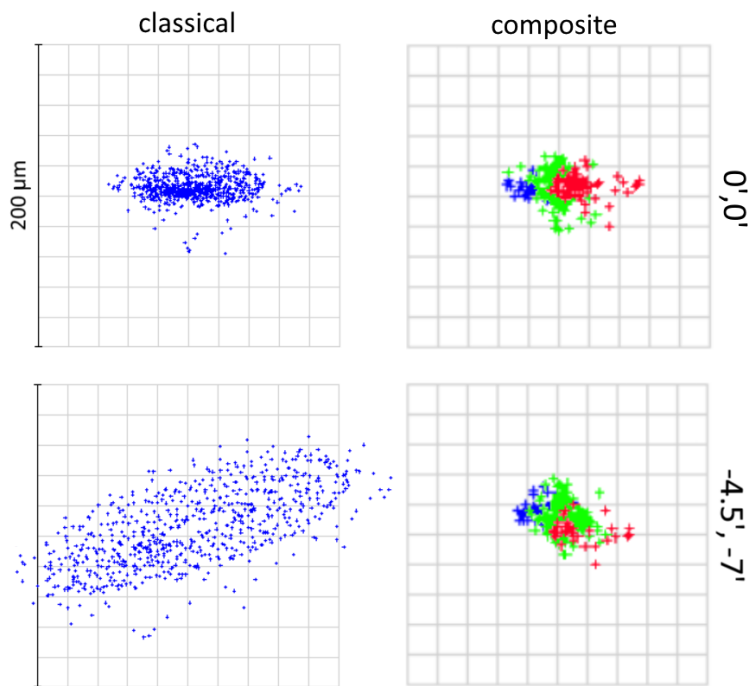


Figure 7. Comparison of the spot diagrams with composite and classical grisms at 650 nm.

The illustrative comparison of the spot diagrams at 650 nm in the FoV center and corner is shown in Fig. 7. In the center the spot sizes are relatively close with RMS radii of 25.8 and 16.3  $\mu m$  for the classical and composite

grism, respectively. In the meantime, in the FoV corner the difference becomes much more significant - 61.5 and 20.7  $\mu m$ , thus making up a gain of factor of 2.97.

Similarly, we compare the DE distributions for the two points of field at 650 nm. The spatial distribution maps are shown in Fig. 8. The Difference is even more notable than for the image quality metrics. The RMS DE value in teh center is 22.5% and 56.2% for the classical and composite hologram, respectively. The corresponding values in the FoV corner are 12.6% and 53.4%.So the maximum gain in the efficiency reaches a factor of 4.2. One can note that a signifiacnt part of the classical grism surface has a very low DE due to the local angles variation, while in the composite elements the "dark" part corresponds to another zone, where the hologram parameters are locally optimized.

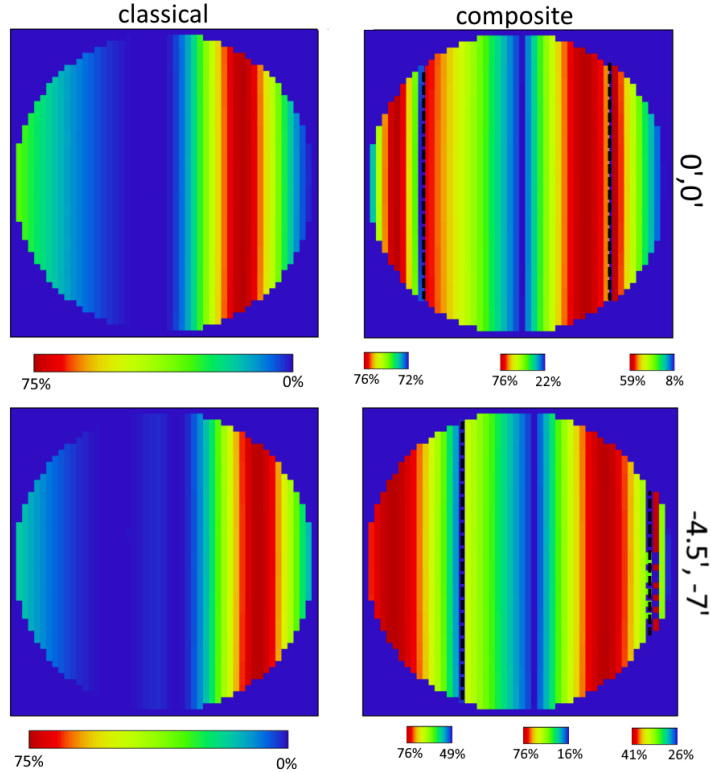


Figure 8. Comparison of the DE distribution with composite and classical grisms at 650 nm.

This simple comparison shows that use of a composite grism promises a great advantage in performance. Obviously, it makes the dispersive element more technologically challenging. But similar spherical grisms with tailored aberrations and efficiency are already known in the field of astronomical instrumentation.<sup>12, 13</sup> So, the main difference in this case consists of the splitting of the element into zones, which should be feasible with the current level of technologies.

## 6. CONCLUSIONS

In the current paper we proposed a low-resolution spectrograph for the CASTLE - a small robotic , which is under development at Laboratoire d'Astrophysique de Marseille. The spectrograph consists of a single element - a composite grism, which represents a volume-phase holographic grating split into 3 zones with locally optimized efficiency and aberrations, imposed on the front surface of a spherical waveguide. The dispersive element is mounted on the telescope filter wheel, and the spectroscopic mode uses the capabilities of the existing detector and focusing mechanism.

Our modelling demonstrates that in a slitless mode it will be able to create spectra over  $9' \times 14'$  field of view and 350-950 nm spectral range with the spectral resolving power up to R690. The diffraction efficiency reaches 64.1%. In comparison with a classical grism we obtain a gain up to 3 times in terms of the image quality and 4.2 times in terms of the efficiency.

The design concept promises to extend the scientific value of the telescope's observations. However, its' practical implementation requires further studies, including verification with advanced numerical modelling methods, adjustment of the optimal design parameters with those achievable with real photosensitive materials, deformable mirrors etc.; performing tolerance analysis, optimizing the mechanical design and including internal baffles.

## ACKNOWLEDGMENTS

Work of E.M., D.A. and D.K. was funded by the Russian Science Foundation grant number 21-79-00082.

## REFERENCES

- [1] Lombardo, S., Muslimov, E., Lemaitre, G., and Hugot, E., "Next-generation telescopes with curved focal surface for ultralow surface brightness surveys," **488**, 5057–5064 (Oct. 2019).
- [2] Grange, R., Milliard, B., Flamand, J., Pauget, A., Waultier, G., Moreaux, G., Rossin, C., Viton, M., and Nevriere, M., "GALEX UV grism for slitless spectroscopy survey," in [*Society of Photo-Optical Instrumentation Engineers (SPIE) Conference Series*], *Society of Photo-Optical Instrumentation Engineers (SPIE) Conference Series* **10569**, 1056908 (Nov. 2017).
- [3] Muslimov, E., Pavlycheva, N., Guskov, I., Akhmetov, D., and Kharitonov, D. Y., "Spectrograph with a composite holographic dispersive element," in [*Society of Photo-Optical Instrumentation Engineers (SPIE) Conference Series*], *Society of Photo-Optical Instrumentation Engineers (SPIE) Conference Series* **11871**, 1187112 (Sept. 2021).
- [4] Lemaitre, G., "Reflective Schmidt anastigmat telescopes and pseudo-flat made by elasticity," *Journal of the Optical Society of America (1917-1983)* **66**, 1334–1340 (Dec. 1976).
- [5] Hugot, E., Jahn, W., Chambion, B., Nikitushkina, L., Gaschet, C., Henry, D., Getin, S., Moulin, G., Ferrari, M., and Gaeremynck, Y., "Flexible focal plane arrays for UVOIR wide field instrumentation," in [*High Energy, Optical, and Infrared Detectors for Astronomy VII*], Holland, A. D. and Beletic, J., eds., *Society of Photo-Optical Instrumentation Engineers (SPIE) Conference Series* **9915**, 99151H (Aug. 2016).
- [6] Chambion, B., Gaschet, C., Behaghel, T., Vandeneynde, A., Caplet, S., Gétin, S., Henry, D., Hugot, E., Jahn, W., Lombardo, S., and Ferrari, M., "Curved sensors for compact high-resolution wide-field designs: prototype demonstration and optical characterization," in [*Photonic Instrumentation Engineering V*], Soskind, Y. G., ed., *Society of Photo-Optical Instrumentation Engineers (SPIE) Conference Series* **10539**, 1053913 (Feb. 2018).
- [7] Peterson, J. R., Jernigan, J. G., Kahn, S. M., Rasmussen, A. P., Peng, E., Ahmad, Z., Bankert, J., Chang, C., Claver, C., Gilmore, D. K., Grace, E., Hannel, M., Hodge, M., Lorenz, S., Lupu, A., Meert, A., Nagarajan, S., Todd, N., Winans, A., and Young, M., "Simulation of Astronomical Images from Optical Survey Telescopes Using a Comprehensive Photon Monte Carlo Approach," **218**, 14 (May 2015).
- [8] Kashikawa, N., Aoki, K., Asai, R., Ebizuka, N., Inata, M., Iye, M., Kawabata, K. S., Kosugi, G., Ohyama, Y., Okita, K., Ozawa, T., Saito, Y., Sasaki, T., Sekiguchi, K., Shimizu, Y., Taguchi, H., Takata, T., Yadoumaru, Y., and Yoshida, M., "FOCAS: The Faint Object Camera and Spectrograph for the Subaru Telescope," **54**, 819–832 (Dec. 2002).
- [9] Muslimov, E. R., Akhmetov, D., Kharitonov, D., Guskov, I., and Pavlycheva, N. K., "Composite waveguide holographic display," in [*Optics, Photonics and Digital Technologies for Imaging Applications VII*], Schelkens, P. and Kozacki, T., eds., **12138**, 209 – 219, International Society for Optics and Photonics, SPIE (2022).
- [10] Lakshminarayanan, V. and Fleck, A., "Zernike polynomials: A guide," *Journal of Modern Optics* **58**(7), 1678–1678 (2011).
- [11] Kogelnik, H., "Coupled wave analysis for thick hologram gratings," *Bell Syst. Tech. J.* **48**, 2909–2947 (1969).

- [12] Kuin, N. P. M., Landsman, W., Breeveld, A. A., Page, M. J., Lamoureux, H., James, C., Mehdipour, M., Still, M., Yershov, V., Brown, P. J., Carter, M., Mason, K. O., Kennedy, T., Marshall, F., Roming, P. W. A., Siegel, M., Oates, S., Smith, P. J., and De Pasquale, M., “Calibration of the Swift-UVOT ultraviolet and visible grisms,” **449**, 2514–2538 (May 2015).
- [13] Caillat, A., Costille, A., Pascal, S., Rossin, C., Vives, S., Foulon, B., and Sanchez, P., “EUCLID/NISP GRISM qualification model AIT/AIV campaign: optical, mechanical, thermal and vibration tests,” in [*Society of Photo-Optical Instrumentation Engineers (SPIE) Conference Series*], *Society of Photo-Optical Instrumentation Engineers (SPIE) Conference Series* **10562**, 1056203 (Sept. 2017).